Remarkable PDMS/PET satin composite transverse pneumatic artificial muscles that are environmentally friendly

Dr.Seelam Jamala Reddy[1], Etikala Sainath[2], L.Vinith Kumar[3],
Associate Professor[1],Assistant Professor [2],
Student[3],
Department of Mechnical,
BRILLIANT GRAMMAR SCHOOL EDUCATIONAL SOCIETY'S GROUP OF INSTITUTIONS-INTEGRATED CAMPUS
Abdullapurmet (V), Abdullapurmet (M), R.R Dt. Hyderabad-501505.

ABSTRACT

New transverse pneumatic artificial muscles (TPAM) are introduced here; they are constructed out of a composite material consisting of a poly (dimethylsiloxane) (PDMS) matrix membrane and a poly (ethylene terephthalate) (PET) satin reinforcement. The internal braid (IB) and external braid (EB) of a miniature TPAM are both flexible and serve to reinforce the membrane. With EB fibbers aligned perpendicular to the IB are positioned on the side. PDMS/PET composite's suitability for uses in the human gastrointestinal tract was investigated (chemical resistance, temperature characteristic), and the performance of variously manufactured TPAMs as actuators for robot driving was tested. The process of PDMS impregnation of PET satin and the influence of immersion in a chosen solution were studied by comparing FT-IR spectra of the composite. Superior biocompatibility can be shown in the composite, and when compared to other pneumatic artificial muscles (PAM), the muscles perform admirably in terms of static load. These findings provide hope for a future in which a painless robot inspection of the digestive system is achievable.

INTRODUCTION

Every robot needs a reliable drive system. Pneumatic, hydraulic, and the most common kind of electric drive are all options for robot propulsion. Hydraulic and pneumatic actuators play a vital part in the functioning of robots and are not only a secondary source of energy. Pneumatic systems include three main components: the air preparation system, the control system, and the actuators. The pneumatic cylinders that transform the pressure energy generated by the working medium into mechanical energy of linear, angular, or curved motion are known as actuators. Pneumatic Artificial Muscle (PAM) is a fascinating actuator that uses pneumatics. PAM is built from a membrane-reinforced flexible braid element. Fi ttings connected to the membrane allow the transmission of mechanical power along the muscle. PAMs are actuators that use a working medium injected into the membrane, most often compressed air. Inhaling the gas causes the muscle to expand, and exhaling it causes the muscle to constrict (Fig. 1). Changing the amount of pressure applied to a muscle may alter the amount of force produced by the muscle1.

The McKibben muscle is the most popular and well-known form of artificial muscle.

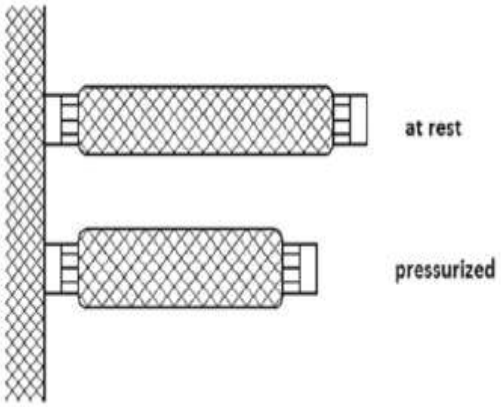

Figure 1. Working of PAM

Rubber bladder reinforced with a nylon braided mesh yarn for rigidity. Compressing air into a muscle induces a radial and longitudinal membrane deformation. Each muscle has a fi tting at its end that, when contracted, generates movement and a pulling force. The operating pressure range for McKibben muscles is 0.1 MPa to 0.5 MPa. The membrane's material strength establishes the upper limit on pressure, since the membrane may be damaged by a working medium that exerts too much force. Muscle force is also affected by the working medium's pressure; with greater pressure, greater levels of force may be generated2.

Pleated articular musculature is a kind of skeletal muscle. These muscles have a membrane with an embedded core that carries tension and are thus

classified as braided muscles. The membrane is folded several times throughout its length. By introducing the working medium to the muscle, the pleated material smoothes out the muscle's fibers and substantially reduces its length, while also providing a substantial increase or decrease in circumference. The maximum length to minimum diameter ratio, membrane deformation, and a predetermined pressure of the compressed air3, 4 all play a role in defining these muscles' unique properties. Young Kwun Lee and Isao Shimoyama's micromuscles mimic the structure of McKibben muscles. They were created in tandem with Samsung throughout the artificial hand's development. Micro muscles, between 18 and 30 centimetres in length and 1 millimetre in diameter, were developed for the drive to simulate the action of a human hand. The internal braid (IB) of a miniature transverse PAM (TPAM) is flexible, whereas the exterior braid (EB) is rigid. The EB is positioned laterally because its fibers run perpendicular to the IB. As can be seen in Figure 2a, the IB assumes a U form while at rest. As can be seen in Figure 2b, when gas is injected into a muscle, the IB expands and takes on a cylindrical form. The change in IB's form indicates shorter distances between EB's extremities. End fittings on an EB transmit mechanical power transversely, allowing for displacement without altering the muscle's length7.

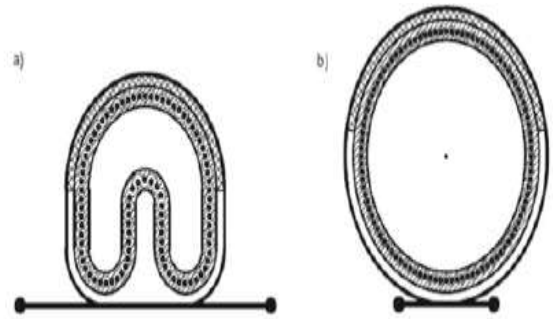

Figure 2: The TPAM's Form Before and After Inflation of Pressurized Air Due to the Possibility of Obtaining a Wave Motion

They are one of the first to employ TPAM as part of the design of a robot's propulsion system for studying the human digestive tract. The muscles' diminutive size is an added perk. In the event of a muscle tear, this is crucial information to have. The patient will not be harmed if the pressure control device ruptures while in use.

Our ultimate objective was to get TPAM constructed from biocompatible materials that also perform as anticipated in terms of maintaining normal muscle activity. New possibilities for several biological and medicinal uses have arisen thanks to recent developments in biomaterials and robotics. In this context, poly (dimethylsiloxane) (PDMS) is an excellent material choice. PDMS has been widely used because of its many useful characteristics. The strongly cross linked PDMS is resistant to heat and most chemicals. PDMS's biocompatibility and no toxicity stem from the fact that it is chemically inert. Modifiable mechanical qualities (through cross-linking agent mixing ratio), simple production, cheap cost, and commercial availability of PDMS are also noteworthy. PDMS also benefits from being homogenous and isotropic, having a porous structure, and having a hydrophobic surface, among other features. The biocompatibility of other polymers may be improved by including PDMS. For medical devices like defibrillator and pacemaker leads, Chaffi n et al. employed PDMS and polyether soft segments in segmented polyurethane multiblock polymers to create robust and readily processed thermoplastic elastomers (PDMS-urethanes). PDMS is also a desirable component in robots. Passive membranes were constructed using PDMS with a 3% glass bubble concentration for neutral buoyancy on the pectoral fins of manta ray robot10. The gecko-like climbing robot11 is another example of a bio-inspired machine; it uses sticky PDMS footpads to stick to surfaces. A small body of literature addresses PDMS-based pneumatic and hydraulic actuators. In order to create PAM, Martinez et al. combined PDMS with Ecofl ex 00-30 (another silicone elastomeric). Internal cores with pneumatic channels benefitted more from the rigidity of PDMS than Ecofl ex. Pneumatic micro fingers, which comprise a micro hand, were created using yet another PDMS pneumatic actuator. The fingers were constructed from two sheets of PDMS with a balloon chamber in the middle. When the chamber expands, it causes the fingers to flex 13. Yoshida et al. also created an electro-rheological fluid (ERF) micro gripper as a different kind of actuator. The PDMS moveable chamber was selected because to the material's flexibility and chemical resistance against working fluids.

Poly (ethylene terephthalate) (PET) also demonstrates biological and chemical inertness, making it a useful polymer. Research on PET fibbers confirms their high heat quality of construction and durability. The melting point of PET fibbers is 245 degrees Celsius, and its tensile modulus reaches 2.21 gigapascals at 15 percent strain. Because of their unique set of characteristics, PET fibers are a promising option for use as reinforcement in composites. Hexapod crawling robots with an fl exude layer16 and flying robots with a 0.2 mm frame of wings17 are also examples of PET reinforcement in action.

Pneumatic actuators like PneuFlex18 employ PET fibbers as reinforcement. PneuFlex is housed inside a helix of PET reinforcement, which maintains the actuator's constant diameter. Fatigue life studies

revealed intriguing findings, demonstrating that PET bladder with latex for pneumatic actuators (Clean-cut®) may endure over 10,000 cycles19.

MATERIAL

Aldrich, a company based in the United States, provided both the PDMS (with a viscosity of 50,000 costs) and the tetraethyl orthosilicate (TEOS) (of reagent grade). We splurged on some PET satin. Originating in China at the Jiaxing Dongtai Textile Factory. All reagents for the preparation of simulated body fl uid (SBF), simulated stomach acid (SSA) and solution of sodium bicarbonate with pH of pancreatic juice (SPJ) - NaCl, NaHCO3, KCl, K2HPO4 . 3H2O, MgCl2. 6H2O, HCl, CaCl2, Na2SO4 and 2-amino-2-hydroxymethyl-propane- 1.3-diol - were supplied from Aldrich, USA of reagent grade. The muscle glue used was ethyl 2-cyanopropenoate, and it was acquired under the brand name Loctite 495 (Henkel, Germany).

EXPERIMENTAL

Preparation of PDMS/PET samples for biocompatibility tests (chemical resistance, thermal characteristics and FT-IR)

Our TPAMs were used to model the location of layers in the samples used for biocompatibility testing. PDMS and TEOS were combined in a variety of Poured into stainless steel molds (mold size - 10.0 0.2 x 10.0 0.2 x 5.0 0.2 mm) at a weight-to-volume ratio of (100:2.6), (100:5.0), and (100:10). When the PDMS matrices had become sufficiently viscous to keep the PET satin pieces on the surface of the matrix (after 30-40 minutes), the correct square pieces (10.0 0.2 x 10.0 0.2 mm) were inserted in each mold. The remaining PDMS: TEOS mixture was poured into the mold to fill it to its furthest depth. Before being sealed, a PDMS/TEOS combination was additionally injected into PET satin. The PDMS matrix cross-linking process was performed at room temperature and pressure. After 24 hours, samples were taken out of the molds. Figure 3 displays the shape of the acquired samples. Figure 4 shows a cross-sectional optical microscope view of a prepared sample.

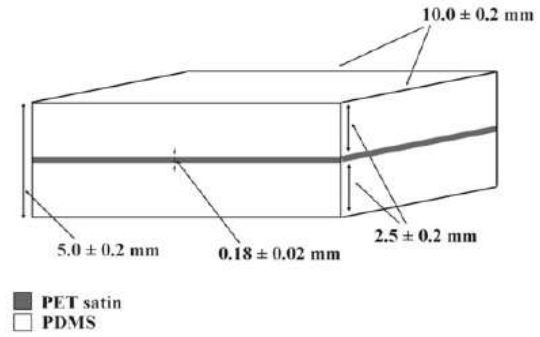

Figure 3. Shape of sample for biocompatibility tests

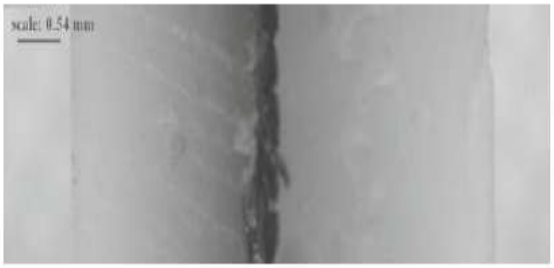

Figure 4. Optical microscopy image of sample's cross-section

Chemical resistance

The ASTM D 543-87 method21 was used to investigate the chemical resistance of PDMS/PET. Human body fluids were simulated by preparing three solutions of varying pH. SSA is a hydrochloric acid solution with a pH of 1.5, designed to mimic stomach acid. The influence of basic pancreatic juice may be estimated by using SPJ with a pH of 8.4. Using the recipe22 developed by Ohtsuki et al., SBF can mimic the ion concentration seen in human blood plasma. The aforementioned solutions were used to weigh and submerge PDMS/PET samples. Samples were exposed to the chosen chemicals for 48 hours, then dried and weighed again. The following formula was used to calculate the percentage of weight change:

Six samples were taken of each solution and their average weight change due to PDMS/TEOS was calculated.

Thermal characteristics

The HDTVICAT 3-300 apparatus (Zwick/Roell, Germany) and the CC-300BX bridge thermostat (Huber, Germany) were used to measure and record temperatures. Thermal ISO 306 norm for Vicat softening temperature (VST) measurements were conducted using method A120 (10 N load, 120°C/h heating rate). The temperature at which a 1 mm2 round steel needle can be inserted into the test sample under a defined stress is used to calculate the VST. The optimal range for sample thickness is 3–6.5 mm. The thickness of our samples was 5.0

0.2 mm, and they were reinforced with PET satin to a depth of 2.5 0.2 mm, measured from the surface of the sample. Needle jamming in the reinforcement (for depths less than 1 mm) was taken into account when deciding where to place the PET satin. Six samples of each PDMS/TEOS combination had their thermal parameters averaged across a range of 30-130 degrees Celsius. The protocol for the manufacture of samples for biocompatibility testing also included reference samples constructed of cross-linked PDMS matrix without PET reinforcement.

Fourier transforms infrared spectroscopy (FT-IR)

Air was used to collect the FT-IR spectra using an FT-IR 175C spectrophotometer (BIORAD, USA). PDMS and PET spectra after cross-linking A sample of composite satin was weighed before and after being submerged in the solutions to compare the results. The impact of impregnation with a PDMS/TEOS combination was also studied by measuring the spectrum of PET satin before and after the treatment.

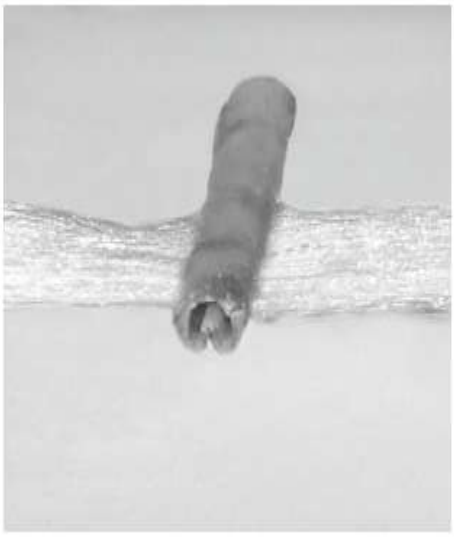

Figure 5. Final shape of the muscle

In addition, the muscle's design must prevent the internal braid from being accidentally displaced. In order to establish a long-lasting link between inside and outside connect the braids together; braiding. It was made by coating the braids in PDMS and then forcing another layer of PDMS between them before sealing the mold.

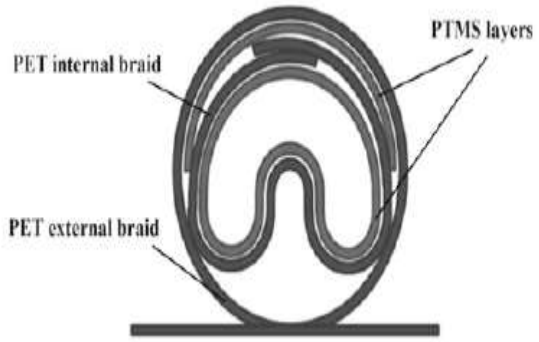

Figure 6. TPAM with an overlap

The second building was uniform, without an internal and external braid. One continuous piece of material was used to create the muscle. Cross-pollination of plaiting the braid material yielded both the interior braid and the link to the outer braid seen in Figure 6. This method prevents the interior braid from shifting uncontrollably and makes the structure more solid. The structure is straightforward to construct, and successful PDMS impregnation of the braids is guaranteed.

Static load characteristics

In order to choose the most efficient muscle architecture, experimental studies of contraction were done. Muscles were exerted.

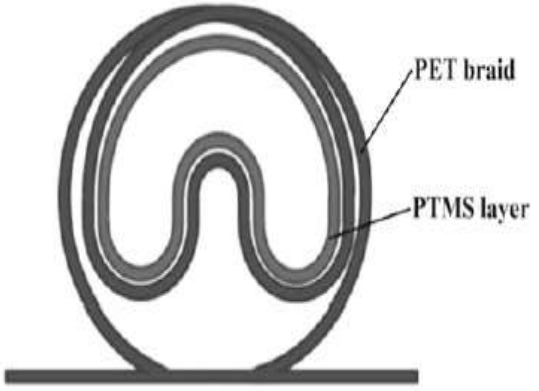

Figure 7. Uniform construction of TPAM

2.5 millimetres in diameter and 10 millimetres in length. Pressure, external strain, and volume-to-length change all played a role in a TPAM's degree of shortening. Related to the muscle. As a result, a study was conducted to determine the relationships between muscle shape change force F and muscle shrinkage h under constant pneumatic pressure of P = 0.1; 0.2; 0.3; 0.4 MPa. The force produced by the muscle upon tensioning the EB was measured and analyzed over a range of pressures. Three tests were performed on each sample. The features of

static loads were mapped out based on the data that was recorded.

RESULTS AND DISCUSSION

Chemical resistance of PDMS/PET

We evaluated the typical shifts in mass for 9 distinct permutations on sample make-up and solvent (Table 1). The purpose of this comparison was to guarantee, that PDMS/PET can withstand the acids and bases in stomach acid. In terms of SSA, SBF, and SPJ chemical resistance, all samples are either very good or exceptional. No increase or decrease in body mass occurs that is more than 0.7% of the weight of the first sample. This is a really impressive finding since, in practical applications, the material will not be subjected to contact with the studied solutions for such a prolonged period of time. Samples with a PDMS:TEOS (100:10) ratio showed the largest average weight changes, perhaps because the PDMS matrix was more susceptible to aqueous solutions due to the extra TEOS.

Although PDMS: TEOS (100:10) has a respectable amount of chemical resistance, it will be abandoned in future research in pursuit of even greater bio resistance.

Thermal characteristics

All compositions' thermal properties were studied between 30 and 130 degrees Celsius (Fig. 8). This spectrum was stretched beyond its natural limits. To enable for a suitable calculation of the boundary conditions for the functioning composite, standard temperatures of the human body and the greatest temperature occurring during the work of artificial muscles are taken into account. We matched our findings to those obtained from a reference sample devoid of PET satin to draw these conclusions.

Table 1. Three PDMS/PET samples were submerged for 48 hours in one of three solutions, and the resulting weight gains and losses were compared. The PDMS/PET samples had varying compositions of PDMS cross linked with TEOS.

Simulated fluids ↓	PDMS:TEOS weight ratio ↓				
	100:2.6	100:5	100:10		
Simulated stomach acid (SSA)	-0.148% – 0.000%	-0.170% – 0.091%	-0.594% – -0.153%	Range	Weight change (%)
	-0.061%	0.016%	-0.417%	Average	
Simulated body fluid (SBF)	0.000% – 0.857%	-0.194% – 0.000%	-0.493% – -0.304%	Range	
	0.018%	-0.080%	-0.365%	Average	
Solution of sodium bicarbonate with pH of pancreatic juice (SPJ)	-0.078% – 0.863%	-0.356% – 0.079%	-0.820% – -0.181%	Range	
	-0.025%	-0.034%	-0.459%	Average	

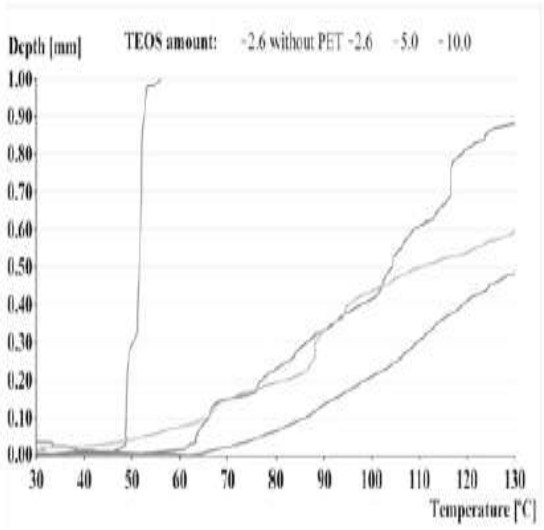

Figure 8 shows the differences in thermal properties between the reference composition without PET satin and those with varying amounts of TEOS. Temperature at which the material softens, often between 230 and 240 degrees Celsius 23. To prevent needle penetration and keep the laminate hermetic, PET satin may also serve as a scaffold. Damage to human GI muscle is very unlikely, although the PDMS: TEOS matrix may be weakened and injured on the outside in exceptional circumstances. Because the PET satin is there, the inner surface is protected, and the material may still function as a pneumatic muscle. When TEOS is added to the PDMS matrix, the laminate's heat resistance improves. All PET satin-containing formulations have a glass transition temperature (GTT) greater than 130 degrees Celsius, indicating that they are suitable for use in artificial muscles. For this reason, a sample of PDMS: TEOS (100:5) submerged in SBF was selected for FT-IR analysis since it demonstrates the most promising features. The FT-IR spectra were compared to that of unprocessed PDMS: TEOS (100:5). The spectra are compared in Figure 9.Spectra of unprocessed PET satin show main absorption at 2968 cm-1 for aliphatic C-H ant symmetric stretching vibration, 1712 cm-1 for C=O stretching vibration, 1409 cm-1 for aromatic skeletal stretching vibration, 1258 cm-1 for ester group stretching vibration, 1097 cm-1 and 1018 cm-1 for aromatic substitution pattern and 1.4 substitution bands in the skeletal ring, 971 cm-1 for O-CH2 stretching vibration in the Additionally, the 1341 cm-1 band (trans conformation of C-C bond in OCH2CH2O-moiety) conveys data on the presence or absence of crystalline areas in the PET satin26.The presence of PDMS is shown by observing a change in the spectra of both untreated PET satin and impregnated PET satin. Amplifications of the following peaks have been observed: 2963 cm1 (C-H stretching in CH3), 1258 cm1 (CH3 symmetric bending in Si-CH3, which covers band of C (O)-O

stretching of ester group), 1093 cm1 and 1018 cm1 (Si-O-Si, which covers bands of an aromatic substitution pattern and 1.4-substitution bands in the skeletal ring), and 1018 cm1 and 1093 cm1.

A second, newly discovered peak, at 793 cm-1 (CH3 rocking in Si-CH3), was also shown to be associated with PDMS. The C=O stretching vibration at 1712 cm-1, the aromatic skeletal stretching vibration at 1409 cm-1, and the trans conformation of the C-C bond in the OCH2CH2O-moiety at 1341 cm-1 all have weaker intensities.

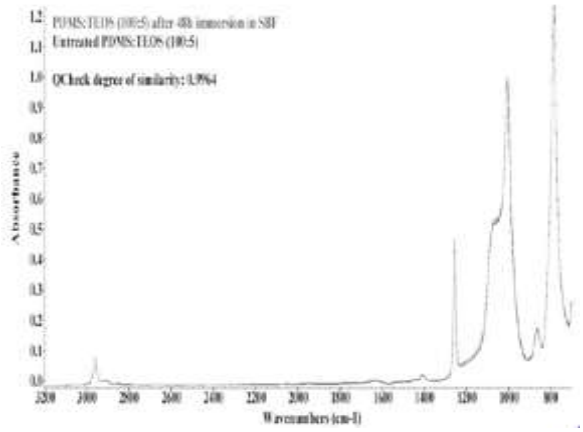

Figure 9 shows a comparison between the FT-IR spectra of untreated PDMS: TEOS (100:5) and PDMS: TEOS (100:5) that was immersed in SBF for 48 hours.

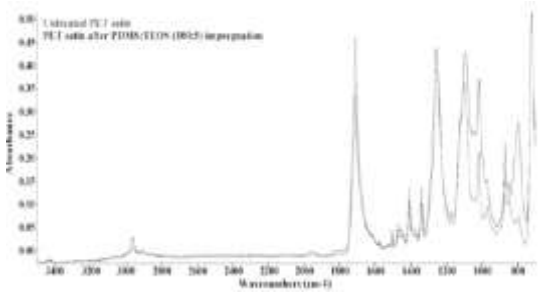

FT-IR spectra of untreated PET satin and PET satin treated with PDMS, shown in Figure 10.Interaction of PDMS methyl groups with PET27 carbonyl and aromatic groups, as well as likely amine groups, is shown by TEOS (100:5) impregnation. Results in the annihilation of -O-CH2-CH2-O- molecules. The results of a comparison between impregnated PET satin and a control sample submerged in SBF are shown in Fig. 11.

The degree of spectral similarity between and was 0.9778 on QCheck. In spite of the spectral changes introduced by the SBF solution, this finding validates PET satin's status as a highly bio resistant material. Peak heights also drop and grow, although just marginally less so.

Static load characteristics

Static characteristics of PAM with core and PDMS (PDMS core) overlap are shown in Figure 12. Muscle deformation is simple and little pressure is all that's required. In order to get really large contraction values. The percentage of shrinkage at 0.1 MPa is 39%, whereas at 0.4 MPa it is 55%. Muscles can only produce a little amount of force, at most 5.9 N at 0.4 MPa.Figure 13 displays the static characteristic of TPAM with an overlapping core attached with ethyl 2cyanopropenoate (glued core), which results in greater force values. When the values of shrinkage are 36% for 0.1 MPa and 41% for 0.4 MPa, the stronger stiffness, which allows attaining larger values of forces, also influences contraction. A constant property of uniform TPAM is shown in Figure 14. Compared to TPAMs with a bonded core, this design enables for larger pressure levels to be obtained (by as much as 46% at 0.4 MPa) while generating forces that are comparable to, if not higher than, those created by this solution.

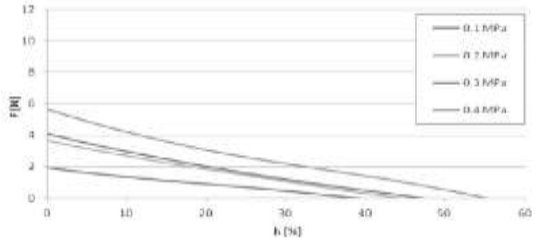

Figure 12. Static characteristic of TPAM with PDMS core

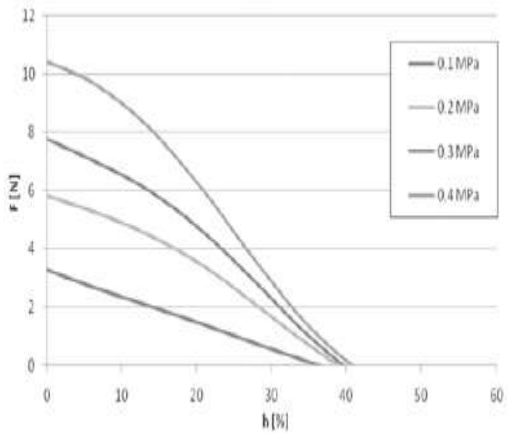

Figure 13. Static characteristic of TPAM with glued core

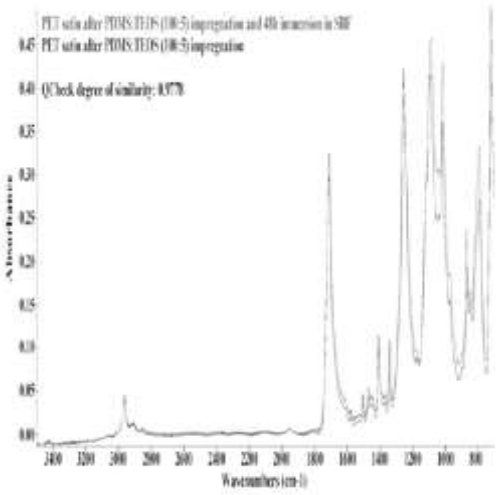

FT-IR spectra of PET satin before and after PDMS: TEOS (100:5) impregnation and 48 hours of immersion in SBF are shown in Figure 11.

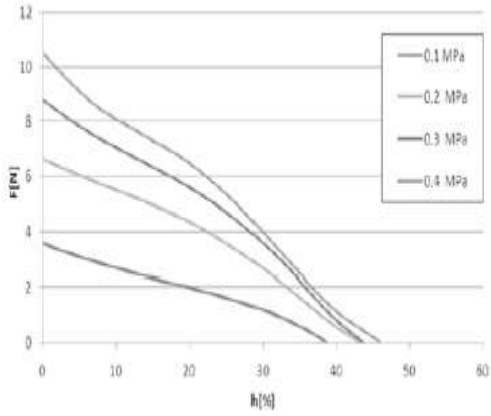

Figure 14. Static characteristic of uniform TPAM

CONCLUSIONS

As a biocompatible composite, PDMS/PET works very well. Both the chemical (FT-IR) and thermal-mechanical (TGA) resistance of the material attested to its biocompatibility. Qualities (thermal and static load) of it. While PDMS ensures chemical inertness and air tightness, PET provides strength and insulation. When it comes to biocompatibility, PDMS/PET with a 100:5 PDMS: TEOS weight ratio is the optimum composite. Thanks to the FT-IR spectra, the impregnation process and chemical resistance could be studied in greater depth. The examination did not reveal any issues with the composite's biocompatibility. The levels of force and shrinkage achieved while filling a muscle with compressed air are dependent on the muscle's anatomy. Overlapping solutions benefit from technological influence, allowing for large pressures or shrinking to be achieved. Uniform TPAM, the final approach, provides the best outcomes by simultaneously achieving high values of forces and shrinkage. In addition, the tightness of the construction afforded by this answer eliminates the possibility of an uncontrolled dislocation of the inner braid or a muscle rupture. When designing medical robots, TPAMs' structure, size, and biocompatibility make them a viable option.

REFERENCE

1. Daerden, F. & Lefeber, D. (2002). Pneumatic artifi cial muscles: actuators for robotics and automation. Eur. J. Mech. Environ. Eng. 47(1), 10–21.

2. Chou, C.P. & Hannaford, B. Measurement and modeling of McKibben Pneumatic Artifi cial Muscles. (1996). IEEE Trans Robot Autom. 12(1), 90–102. DOI: 10.1109/70.481753.

3. Daerden, F. & Lefeber, D. (2001). The concept and design of Pleated Pneumatic Artifi cial Muscles. Int. J. Fluid. Power. 2(3), 41–50. DOI: 10.1080/14399776.2001.10781119.

4. Villegas, D., Van Damme, M., Vanderborght, B., Beyl, P. & Lefeber, D. (2012). Third-Generation Pleated Pneumatic Artificial Muscles for Robotic Applications: Development and Comparison with McKibben Muscle. Adv. Robot. 26(11–12), 1205–1227. DOI: 10.1080/01691864.2012.689722.

5. Lee, Y.K. & Shimoyama, I. (2002, January). A multi--channel micro valve for micro pneumatic artifi cial muscle. In Micro Electro Mechanical Systems, 2002. The Fifteenth IEEE International Conference on (pp. 702–705). IEEE.

6. Lee, Y.K. & Shimoyama, I. (1999). A skeletal framework artificial hand actuated by pneumatic artifi cial muscles. In Robotics and Automation, 1999. Proceedings. 1999 IEEE International Conference on (Vol. 2, pp. 926–931). IEEE.

7. Koter, K., Podsedkowski, L. & Szmechtyk, T. (2015, July). Transversal Pneumatic Artifi cial Muscles. In Robot Motion and Control (RoMoCo), 2015 10th International Workshop on (pp. 235–239). IEEE. DOI: 10.1109/RoMoCo.2015.7219741.

8. Zhou, J., Ellis, A.V. & Voelcker, N.H. (2010). Recent developments in PDMS surface modifi cation for microfl uidic devices. Electrophoresis 31(1), 2–16. DOI: 10.1002/elps.200900475.